Detecting Fragmentation of Kidney Stones in Lithotripsy by Means of Shock Wave Scattering

Oleg A. Sapozhnikov*†, Leonid A. Trusov*, Neil R. Owen†, Michael R. Bailey†, and Robin O. Cleveland‡

*Department of Acoustics, Faculty of Physics, M.V. Lomonosov Moscow State University, Leninskie Gory, Moscow 119992, Russia
†Center for Industrial and Medical Ultrasound, Applied Physics Laboratory, University of Washington, 1013 NE 40th Street, Seattle, Washington 98105, USA
‡Department of Aerospace and Mechanical Engineering, Boston University, 110 Cummington Street, Boston, Massachusetts 02215, USA

Abstract. Although extracorporeal shock wave lithotripsy (a procedure of kidney stone comminution using focused shock waves) has been used clinically for many years, a proper monitoring of the stone fragmentation is still undeveloped. A method considered here is based on recording shock wave scattering signals with a focused receiver placed far from the stone, outside the patient body. When a fracture occurs in the stone or the stone becomes smaller, the elastic waves in the stone will propagate differently (e.g. shear waves will not cross a fracture) which, in turn, will change the scattered acoustic wave in the surrounding medium. Theoretical studies of the scattering phenomenon are based on a linear elastic model to predict shock wave scattering by a stone, with and without crack present in it. The elastic waves in the stone and the nearby liquid were modeled using a finite difference time domain approach. The subsequent acoustic propagation of the scattered waves into the far-field was calculated using the Helmholtz-Kirchhoff integral. Experimental studies were conducted using a research electrohydraulic lithotripter that produced the same acoustic output as an unmodified Dornier HM3 clinical lithotripter. Artificial stones, made from Ultracal-30 gypsum and acrylic, were used as targets. The stones had cylindrical shape and were positioned co-axially with the lithotripter axis. The scattered wave was measured by focused broadband PVDF hydrophone. It was shown that the size of the stone noticeably changed the signature of the reflected wave.

Keywords: lithotripsy, kidney stones, acoustic scattering, shock waves
PACS: 43.80.Gx, 87.54.Hk, 43.20.Gp

INTRODUCTION

In shock wave lithotripsy, kidney stones are fragmented by shock waves. The shock waves induce collateral kidney damage, which increases with the number and peak pressure of the shock waves. Currently fragmentation is monitored by fluoroscopy or ultrasound imaging which have limited spatial resolution and do not produce reliable feedback on fragmentation. The consequence is that too many shock waves may be fired, resulting in unnecessary damage to the kidney. Therefore, the development of an accurate method for monitoring stone fragmentation is needed. This would allow a doctor to stop the shock wave application appropriately. Further,

CP829, *Therapeutic Ultrasound: 5th International Symposium on Therapeutic Ultrasound*
edited by G. T. Clement, N. J. McDannold, and K. Hynynen

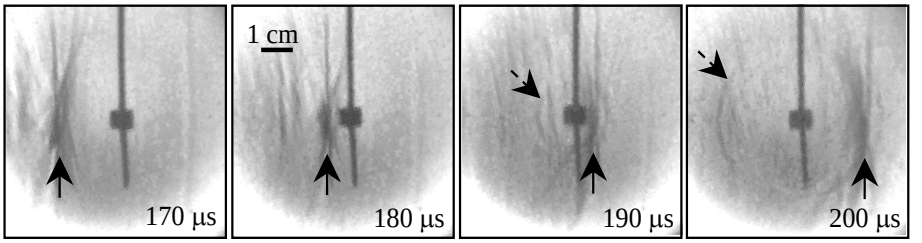

FIGURE 1. Shadowgraphic observation of a lithotripter shock wave scattering from a stone. The images are captured in water with a high-speed camera at different time moments after the shock wave emission. The shadow of the stone (cylindrical shape, 6.5 mm diameter, 8.5 mm length, made from U-30 cement) is seen in the center of the images. Solid arrows show the position of the incident shock wave, which propagates from left to right from an electrohydraulic lithotripter. Dashed arrows indicate the wave scattered by the stone. This scattered wave can be detected far-away from the stone to monitor the stone fragmentation.

one may want to alter shock wave characteristics (e.g., reduce the peak pressure) at certain points in the fragmentation process as the fragmentation process may be sensitive to fragmentation state (e.g., stone size).

In this work a method is presented in which waves scattered by the stone will be detected by a focused receiver, which can be placed far from the stone, for example, on the skin of the patient. The scattering occurs due to acoustic impedance mismatch between the liquid and the stone and reverberation of the shock wave inside the stone. This process is illustrated in Fig.1, where high-speed shadowgraphy of incident and scattered acoustic waves is shown. When a fracture occurs in the stone or the stone becomes smaller, the elastic waves propagate differently (e.g. shear waves do not cross a fracture) which, in turn, changes the scattered acoustic wave in the surrounding liquid. A similar approach, with attention to cavitation emission, was recently proposed by Fedele *et al*. [1].

THEORY

Elastic waves in the stone and surrounding liquid

The kidney stone and surrounding liquid were assumed to behave as linear, isotropic, elastic media, in which case the underlying equations are Newton's Second Law and Hooke's Law:

$$\frac{\partial v_i}{\partial t} = \frac{1}{\rho_0}\frac{\partial \sigma_{ij}}{\partial x_j} \tag{1}$$

$$\frac{\partial \sigma_{ij}}{\partial t} = \lambda \delta_{ij}\frac{\partial v_k}{\partial x_k} + \mu\left(\frac{\partial v_i}{\partial x_j} + \frac{\partial v_j}{\partial x_i}\right) \tag{2}$$

The equations are written in index notation and v_i represent the velocity at each location, σ_{ij} the stress tensor, δ_{ij} the Kronecker delta function, ρ_0 is the material density and λ and μ the Lame coefficients of the material. More details on the model, e.g., initial and boundary conditions, equations in axisymmetric case, and the finite-difference numerical algorithm are described in our previous publications [2, 3].

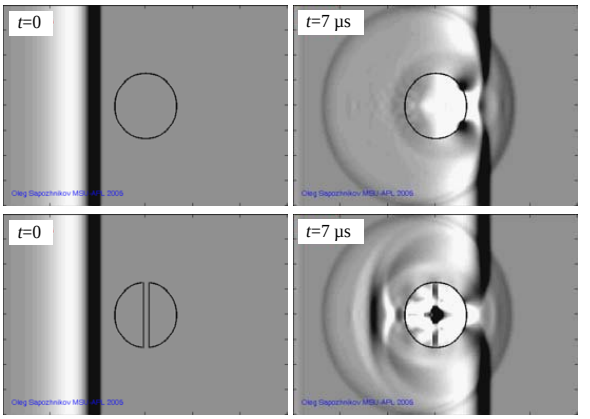

FIGURE 2. Modeling of shock wave scattering a spherical stone. The images on the left-hand side show acoustic pressure distribution before the shock wave arrival to the stone (t=0). The shock wave propagates from left to right; dark and bright regions indicate positive and negative acoustic pressure, respectively. The images on the right-hand side show pressure distribution at 7 μs. The top images correspond to the stone without a crack, the bottom images correspond to the stone that has 0.5-mm thickness liquid-filled crack.

In liquid $\mu = 0$ and acoustic pressure is $p = -\sigma_{kk}/3$. The acoustic scattering phenomenon was modeled for cylindrical and spherical stones with and without crack. The presence of a crack in the stone was simulated by introducing a liquid-filled lateral layer dividing the stone into two pieces. The modeling was performed in a cylindrical region 2 cm diameter and 3 cm length, which was several times larger than the stone (less than 1 cm diameter). Typical results are shown in Fig.2 for a spherical U-30 stone of 6.5-mm diameter. It is clearly seen that the presence of the crack changes the scattered acoustic field.

Scattered wave in liquid far from the stone

The subsequent acoustic propagation of the scattered waves into the far-field (where the receiver is placed) is difficult to model in finite differences because of the large calculation region, more than 10 cm in diameter. To avoid this difficulty, we used the Helmholtz-Kirchhoff diffraction integral that relates the acoustic pressure $p(\mathbf{r}',t)$ and its normal derivative specified on a surface S (denoted by $\mathbf{r}'$) surrounding the scatterer to the acoustic pressure $p(\mathbf{r},t)$ at any point $\mathbf{r}$ outside this surface:

$$p(\mathbf{r},t) = \frac{1}{4\pi}\int_S \left\{ -\frac{1}{R}\frac{\partial p\left(\mathbf{r}', t-\frac{R}{c}\right)}{\partial n(\mathbf{r}')} - \frac{\partial R}{\partial n(\mathbf{r}')}\left[\frac{p\left(\mathbf{r}', t-\frac{R}{c}\right)}{R^2} + \frac{1}{cR}\frac{\partial p\left(\mathbf{r}', t-\frac{R}{c}\right)}{\partial t} \right] \right\} ds' \quad (3)$$

Here $R = |\mathbf{r}-\mathbf{r}'|$, c is speed of sound, and $\partial/\partial n(\mathbf{r}')$ is spatial derivative in the direction of the outer normal to the integration surface. The surface S can be arbitrary, however, in the modeling it is convenient use a cylindrical shape placed close to the stone. The latter allows reducing the calculation region in the previously described finite-difference model. The acoustic pressure $p(\mathbf{r}',t)$ and its temporal and spatial derivatives on the surface S are calculated using finite differences. The far-field pressure $p(\mathbf{r},t)$ was calculated using Eq.(3) at the surface of the acoustic receiver, and the receiving signal was calculated by averaging acoustic pressure over the

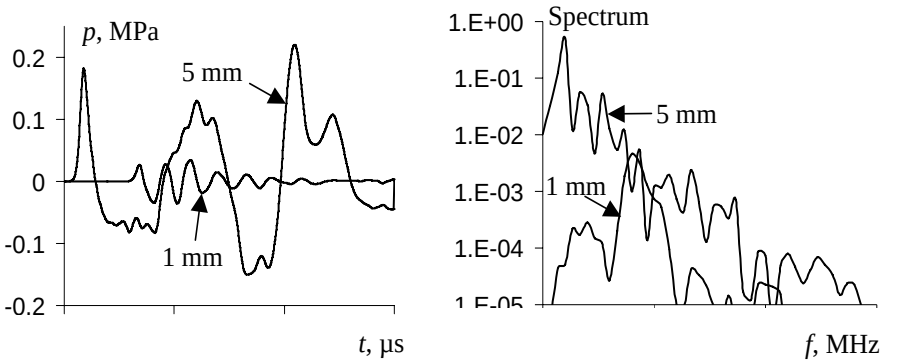

FIGURE 3. Pressure waveform (left) and the corresponding normalized spectrum (right) due to 40 MPa lithotripter shock wave scattering from spherical stones of 1 and 5 mm diameter. Distance from the stone to the hydrophone is 10 cm, observation angle from the lithotripter axis is 150^0.

hydrophone surface. The modeling demonstrates that the presence of a crack in the stone changes the hydrophone signal waveform (data not shown) based on the signals shown in Fig. 1. In addition, stones of different size also resulted in different signals. Figure 3 shows that there are both qualitative and quantitative differences in the signals scattered from 1 and 5 mm stones. In particular, the time-domain signal from the 5 mm stone is longer in duration and has higher amplitude than the signal from the 1 mm stone. In the frequency domain the 5 mm stone has its peak at a lower frequency and also has higher amplitude. The predicted pressure amplitude at a distance of 10 cm from the stone is of the order 0.1 MPa, which is large enough to be detected with conventional ultrasound transducers.

EXPERIMENT

Experimental studies were conducted using a research electrohydraulic lithotripter modeled after an unmodified Dornier HM3 clinical lithotripter (Fig. 4). Artificial stones, made from Ultracal-30 gypsum and acrylic, were used as targets. The stones had cylindrical shape and were positioned co-axially with the lithotripter axis. The

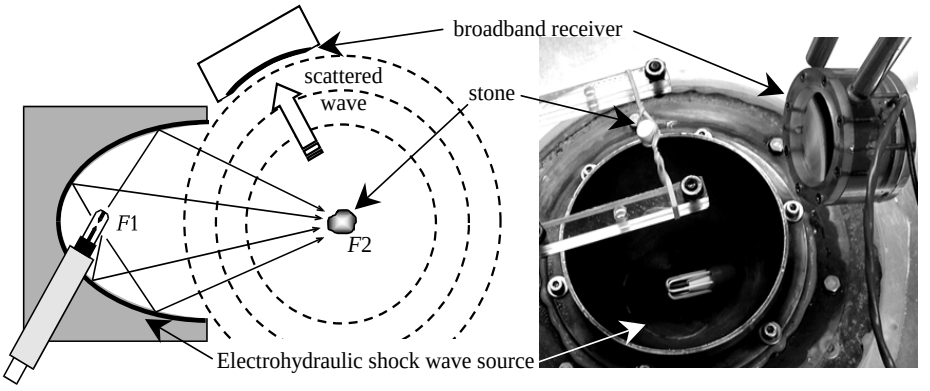

FIGURE 4. Experimental arrangement.

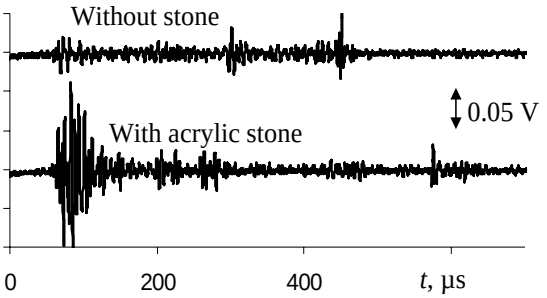

FIGURE 5. Hydrophone signal coming from the focal region of the lithotripter. Spark voltage was 18 kV, distance to the hydrophone was 10 cm. Without the stone, the hydrophone records cavitation signals from the collapsing bubbles. With the stone, a strong signal is observed due to scattering of the shock wave.

acrylic stone was 9.5 mm diameter and 11 mm length. The scattered wave was measured by focused broadband hydrophone made from 25 μm thick PVDF. The hydrophone active element is 5 cm diameter and 10 cm curvature radius. The hydrophone was positioned confocal with the lithotripter. To reduce cavitation, the measurements were performed in degassed water in a single pulse regime. However, cavitation signals were observed even without the stone (Fig. 5). When a stone was placed to the lithotripter focus, the hydrophone voltage increased due to the strong scattering. Cavitation peaks due to inertial collapses remained and typically occurred with longer delay in comparison with the cavitation signal without the stone.

CONCLUSIONS

Scattering of the lithotripter shock wave from kidney stones can be used to monitor some features of the stone fragmentation process. Numerical modeling was used to predict the pressure field around the surface of the stone and the Helmholtz-Kirchhoff integral was used to calculate the pressure wave received at the surface of a remote focused hydrophone. Amplitudes are sufficient for differentiation of signals as stones crack and become smaller. Experiments demonstrate the validity of the proposed approach.

ACKNOWLEDGMENTS

Work supported by NIH DK43881, NIH-Fogarty, CRDF, NSBRI SMS00402, and RFBR. We are thankful to Adam Maxwell and Brian MacConaghy (University of Washington) for designing spherical PVDF hydrophone used in the experimental part of the present work.

REFERENCES

1. Fedele, F., Coleman, A. J., Leighton, T. G., White, P. R., and Hurrell, A. M., "Development of a new diagnostic sensor for Extra-corporeal Shock-Wave Lithotripsy," in Proceedings of the First Conference in Advanced Metrology for Ultrasound in Medicine, *Journal of Physics: Conference Series 1*, 2004, pp. 134-139.
2. Sapozhnikov, O. A., Bailey, M. R., Cleveland, R. O., and Crum, L. A., "Modeling of stresses generated by lithotripter shock wave in cylindrical kidney stone," in Proc. of ISTU3, ed. by J. Y. Chapelon and C. Lafon, INSERM, Lyon, 2003, pp. 323-328.
3. Cleveland, R. O., and Sapozhnikov, O. A., *J. Acoust. Soc. Am.* **118**, 2667-2676 (2005).